An Intelligent Droop Control for Simultaneous Voltage and Frequency Regulation in Islanded Microgrids

Hassan Bevrani, *Senior Member, IEEE*, and Shoresh Shokoohi, *Member, IEEE*

***Abstract*—Voltage and frequency of microgrids (MGs) are strongly impressionable from the active and reactive load fluctuations. Often, there are several voltage source inverters (VSIs) based distributed generations (DGs) with a specific local droop characteristic for each DG in a MG. A load change in a MG may lead to imbalance between generation and consumption and it changes the output voltage and frequency of the VSIs according to the droop characteristics. If the load change is adequately large, the DGs may be unable to stabilize the MG. In the present paper, following a brief survey on the conventional voltage/frequency droop control, a generalized droop control (GDC) scheme for a wide range of load change scenarios is developed. Then to remove its dependency to the line parameters and to propose a model-free based GDC, a new framework based on adaptive neuro-fuzzy inference system (ANFIS) is developed. It is shown that the proposed intelligent control structure carefully tracks the GDC dynamic behavior, and exhibits high performance and desirable response for different load change scenarios. It is also shown that the ANFIS controller can be effectively used instead of the GDC. The proposed methodology is examined on several MG test systems.**

***Index Terms*—ANFIS, DG, droop control, frequency control, microgrid, voltage control.**

I. Nomenclature

ANN	Artificial Neural Network.
ANFIS	Adaptive Neuro-Fuzzy Inference System.
BP	Back-Propagation.
DG	Distributed Generation.
FL	Fuzzy Logic.
FIS	Fuzzy Inference System.
GDC	Generalized Droop Control.
IIDG	Inverter Interfaced Distributed Generation.
I/O	Input/Output.
LSE	Least Square Error.
MF	Membership Function
MG	Microgrid.
MISO	Multi-Input-Single-Output.
PWM	Pulse Width Modulation
RES	Renewable Energy Source.
VSI	Voltage Source Inverter.

Manuscript received May 08, 2012; revised August 27, 2012, November 12, 2012, January 07, 2013, March 02, 2013; accepted April 09, 2013. Date of publication May 01, 2013; date of current version August 21, 2013. This work is supported in part by the Research Office at University of Kurdistan.

H. Bevrani is with the Department of Electrical and Computer Engineering, University of Kurdistan, Sanandaj, Iran.

S. Shokoohi is with the Department of Electrical and Computer Engineering, University of Kurdistan, Sanandaj, Iran and also with the Iranian Oil Pipelines and Telecommunication Company (IOPTC), Khoramabad, Iran (e-mail: bevrani@ieee.org).

Digital Object Identifier 10.1109/TSG.2013.2258947

II. Introduction

THE concepts of microgrid (MG) and distributed generation (DG) are two subjects that have been presented in the areas of electrical distribution systems. A MG is a collection of DGs that are working together for transferring a confident, economical, and environmental power.

Some new challenges on the MGs operation and control such as voltage and frequency control in both connected and islanded modes are presented in [1]–[3]. The impacts of energy storage devices on dynamic MG response are studied in [4]. In connected mode, for regulating voltage and frequency of the MG, the direct-quadrature-current control method is used [5], [6]. Several conventional and intelligent techniques are used for the MG voltage and frequency stabilizing [7]–[12]. Application of Intelligent algorithms such as artificial neural networks (ANNs) in power system control has been frequently used in the literature review [13], [14]. In [15], the ANNs are used for the voltage stability assessment. Using intelligent techniques such as fuzzy logic (FL) and ANNs for control of interconnected power systems generation are reported in [16].

Despite many advantages, the MGs cause some new problems such as changing of power flow pattern, increasing high frequency harmonics due to use of power electronic devices; and increasing frequency and voltage fluctuations due to variable nature of renewable energy sources (RESs) [17]. The RESs are mostly interfaced to the MG by power electronic interfaces such as inverters. In islanding operating mode of MGs, mostly the voltage source inverters (VSIs) are in use [18]. In this case, voltage and frequency of the MG are controlled through local control loops. To avoid circulating currents between parallel inverters connected to MG, usually control strategies based on droop characteristics are applied [19].

Recently, several control techniques have been used to improve the voltage and frequency regulation performance in the

MG systems, mostly using the system droop characteristics. In the previous published works [19]–[25], MGs are usually considered as resistive or inductive systems. In inductive MGs, due to the existence of a strong linkage between reactive power and voltage, the conventional reactive-power/voltage (Q/V) droop control based strategies are used for the voltage control. While, in resistive MGs, the active-power/voltage (P/V) droop control techniques are used for this purpose. Since, the frequency fluctuation is mainly caused by the fluctuation in real power, the active-power/frequency (P/f) droop control methods are used for frequency control. However, since a strong linkage exists between reactive power and grid frequency, the Q/f droop techniques are also needed for MGs frequency control design.

The present paper addresses the simultaneous impacts of active and reactive power fluctuations on the MGs' voltage and frequency. Then based on the well-known droop control relationship, a generalized droop control (GDC) is developed to decuple the active and reactive power impacts on the voltage and frequency. The GDC is a more real droop control and provides a simultaneous voltage and frequency control but it is highly dependent on the line parameters between IIDG and load. In large scale MGs with several inverter interfaced distributed generation (IIDGs), calculating of equivalent line parameters to establish the GDC is difficult.

At the next step, to resolve this problem, a new intelligent droop control using adaptive neuro-fuzzy inference system (ANFIS) is proposed. The ANFIS droop controller can be trained by a proper training set data, so it offers some benefits such as independency from the MG model and structure. The proposed intelligent droop control methodology is also applicable to provide a desirable performance over a wide range of operating conditions.

First, the GDC is tested on a simple MG and the input and output data of the GDC is saved under several severe load changes up to 10% nominal overload. Then, the saved data is used as training data to train the ANFIS unit to behave like a dynamic GDC mechanism. To demonstrate the effectiveness of the proposed control structure, the ANFIS-based GDC is tested on 11-bus and 14-bus MG test systems. The voltage and frequency deviations are studied under violent load changes in different buses. Simulation studies are performed to illustrate the effectiveness of the proposed intelligent control scheme.

This paper is organized as follows: In Section III, a generalized droop control based on inductive and resistive ratio is presented. Then, the generalized droop control is tested on a simple MG with different values of line parameters. In Section IV, The performance and applicability of the approach is improved by replacing the developed GDC with an ANFIS-based intelligent GDC. In Section V, the ANFIS-based control performance is examined on three test systems, and finally, the paper is concluded in Section VI.

III. Generalized Droop Control

A. Conventional Droop Control

Consider a simple MG as shown in Fig. 1. The DG is connected to the load L, with line impedance Z. At point S, as represented in Fig. 1, the active and reactive powers can be expressed as follows [13]:

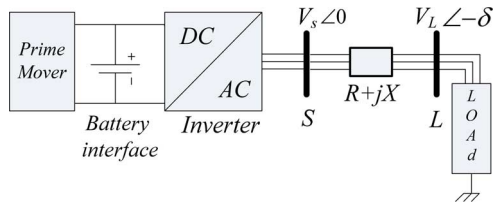

Fig. 1. Simple MG with an interfaced inverter system.

$$P = \frac{V_s^2}{Z}\cos\theta - \frac{V_s V_L}{Z}\cos(\theta+\delta) \quad (1)$$

$$Q = \frac{V_s^2}{Z}\sin\theta - \frac{V_s V_L}{Z}\sin(\theta+\delta) \quad (2)$$

where, θ is the angle of line impedance Z. Considering $\mathrm{Ze}^{\mathrm{j}\theta} = \mathrm{R} + \mathrm{jX}$, (1) and (2) can be rewritten as

$$P = \frac{V_s}{R^2+X^2}[R(V_s - V_L\cos\delta) + XV_L\sin\delta] \quad (3)$$

$$Q = \frac{V_s}{R^2+X^2}[-RV_L\sin\delta + X(V_s - V_L\cos\delta)] \quad (4)$$

Above equations show dependency of the inverter output voltage and power angle δ to the active and reactive powers. Assuming an inductive line $(\mathrm{X} \gg \mathrm{R})$, and a too small power angle results in:

$$\delta = \frac{XP}{V_s V_L}; V_s - V_L = \frac{XQ}{V_s} \quad (5)$$

Equations (5) show that in the inductive MGs, P must be controlled for regulation of δ. While, $\mathrm{V_s}$ is controllable by Q. In other words, in these MGs, the output reactive power controls the inverter voltage, and the active power controls the system frequency, independently. These strategies are known as Q/V and P/f controls, respectively.

Considering above issue, two typical equations can be defined by applying a linear approximation for Q/V and P/f controls:

$$f - f_0 = -k_p(P - P_0) \quad (6)$$

$$V_s - V_{s0} = -k_q(Q - Q_0) \quad (7)$$

where, $\mathrm{f_0}$ and $\mathrm{V_{s0}}$ are rated frequency and voltage of the MG. The k_p and k_q are droop coefficients of DG's active and reactive powers. According to (6) and (7), if a change happens in the frequency or voltage of inverter, for any reason, the impact can be observed on the output active and reactive powers of the inverter. The amount of suitable frequency and voltage deviation can be achieved through the droop characteristics. This primary control provides a fast control action to keep the instantaneous balance between system production and consumption [14], [26].

Despite changes in the frequency and voltage indexes of a pulsewidth modulation (PWM) generator, the MG frequency and voltage are kept in the rated range. But, if the MG is resistive ($\mathrm{X} \ll \mathrm{R}$), then, the (5) should be modified as follows

$$\delta = -\frac{RQ}{V_s V_L}; \quad V_s - V_L = \frac{PR}{V_s} \tag{8}$$

Equations (8) show a strong linkage between reactive power and power angle, as well as between active power and voltage. The frequency regulation automatically controls power angle. Thus, in the resistive MGs, the P/V and Q/f droop control techniques are needed for the voltage and frequency controller synthesis, respectively. These methodologies are based on independency of voltage variation and frequency deviation. While, this two factors (voltage and frequency) are dependent to the line parameters.

B. Generalized Droop Control (GDC)

In a general case, both X and R should be considered [13]. Hence, modified active and reactive powers (P' and Q') are required as follows:

$$P' = \frac{X}{Z}P - \frac{R}{Z}Q \tag{9}$$

$$Q' = \frac{R}{Z}P + \frac{X}{Z}Q \tag{10}$$

Now, defining the index $\mathrm{K_R}$ as $K_R = (R/X)$, and applying (6) and (7) to (9) and (10), results in

$$P' = \frac{X}{Z}[K_f \Delta f + P_0 - K_R K_V \Delta V_s - K_R Q_0] \tag{11}$$

$$Q' = \frac{X}{Z}[K_R K_f \Delta f + k_R P_0 + K_V \Delta V_s + Q_0] \tag{12}$$

where, $\mathrm{K_f} = -1/\mathrm{k_p}, \mathrm{K_V} = -1/\mathrm{k_q}$. The $\Delta\mathrm{f}$ and $\Delta\mathrm{V_s}$ are inverter frequency and voltage deviations, respectively. In (11) and (12), the index $\mathrm{K_R}$ is defined to show what percentage of line is resistive. This index helps us to realize the simultaneous control of voltage and frequency. After some algebraic calculations on (11) and (12), following expressions are obtained.

$$\Delta f = \frac{1}{K_f}\left(\frac{Z}{X}P' - P_0\right) + \frac{K_R K_V}{K_f}\Delta V_s + \frac{K_R}{K_f}Q_0 \tag{13}$$

$$\Delta V_s = \frac{1}{K_V}\left(\frac{Z}{X}Q' - Q_0\right) - \frac{K_R K_f}{K_V}\Delta f - \frac{K_R}{K_V}P_0 \tag{14}$$

From (13), it is denoted that $\mathrm{K_f}$ affects the weighting coefficients of $\Delta\mathrm{V_s}$ and $\mathrm{Q_0}$ in the second and third terms, respectively. Thus, to prevent an undesired effect of $\mathrm{K_f}$ on the $\Delta\mathrm{V_s}$ and $\mathrm{Q_0}$ in the second and third terms of (13), $\mathrm{K_f}$ must be equal to unit. Similarly, in the second and third terms of (14) $\mathrm{K_V}$ should be fixed at unit. Then, it can be seen that from (13) and (14) we can obtain the following generalized droop control relationship:

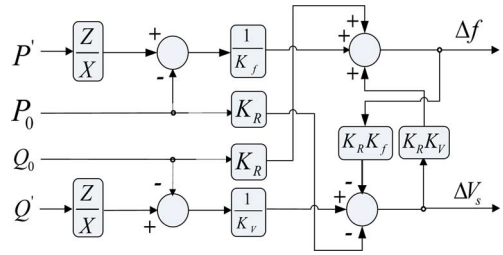

Fig. 2. Block diagram of the GDC.

$$\Delta f = \frac{1}{K_f}\left(\frac{Z}{X}P' - P_0\right) + K_R K_V \Delta V_s + K_R Q_0 \tag{15}$$

$$\Delta V_s = \frac{1}{K_V}\left(\frac{Z}{X}Q' - Q_0\right) - K_R K_f \Delta f - K_R P_0 \tag{16}$$

Fig. 2 shows the block diagram realization of (15) and (16).

C. GDC-Based Voltage and Frequency Control

Fig. 3 shows a general block diagram for a VSI. The LCL output filter has been added to prevent the resonance impact in the output network. Also, the LCL damps the distortion of output sinusoidal waveform and reduces high frequency harmonics caused by switching operations of the VSI. Therefore, it is used in the inverter output for preservation of quality of output current and bus voltage when links to the weak grids [27]. The instantaneous active and reactive powers are passed through low-pass filters, as follows [28].

$$P' = \frac{\omega_c}{s + \omega_c}p; \quad Q' = \frac{\omega_c}{s + \omega_c}q \tag{17}$$

where, ω_c represents the cut-off frequency of low-pass filters. The power controller determines the real and reactive power, and renders P' and Q' to the GDC to perform simultaneous voltage and frequency control proportional to the P' and Q'.

To illustrate the effectiveness of the proposed control strategy, first, the simple test case shown in Fig. 1 is considered. This MG has one DG unit to supply acceptable power for the local load. The load is connected to the DG through a line.

To ensure that the developed droop control strategy is able to obtain a desirable result in inductive, resistive and all types of MGs, some simulations have been done in states of $\mathrm{K_R} = 0.1$ (inductive line: $\mathrm{X} = 10\mathrm{R}$), $\mathrm{K_R} = 1$ ($\mathrm{R} = \mathrm{X}$), and $\mathrm{K_R} = 10$ (resistive line: $\mathrm{R} = 10\mathrm{X}$). The rated voltage and power are 220 V (rms) and 30 kVA, respectively. Main system parameters are shown in Table I.

In Fig. 4, a severe scenario for load variations is considered so that before 0.6 s, the primary load is purely active and is fixed about 0.7 pu. After 0.6 s, for next three steps i.e., 0.6 s, 0.8 s and 1 s, active load is increased. Then, in other three steps at 1.2 s, 1.4 s and 1.6 s, reactive load is increased while active load

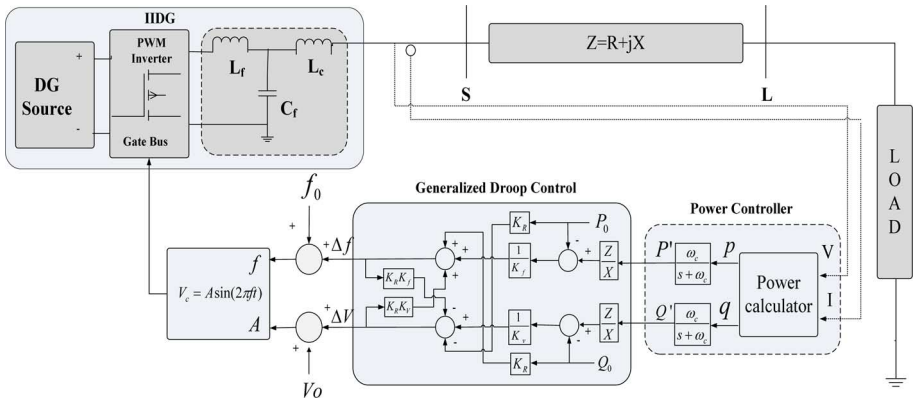

Fig. 3. MG with a general block diagram of VSI.

TABLE I
INVERTER PARAMETERS FOR DGS IN FIG. 3

Parameter	Value	Parameter	Value
$V_{L\text{-}L}$	380 v_{rms}	C_f	30 μF
f	50 Hz	r_{cf}	5 Ω
P_{nom}	30 kVA	L_{Lc}	3mH
f_s	4 kHz	r_{Lc}	0.1 Ω
L_f	6mH	K_f	-1.06
r_f	0.2 Ω	K_v	-100

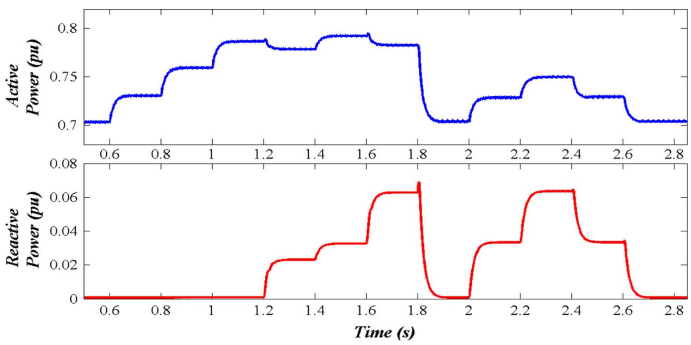

Fig. 4. Load variations scenario.

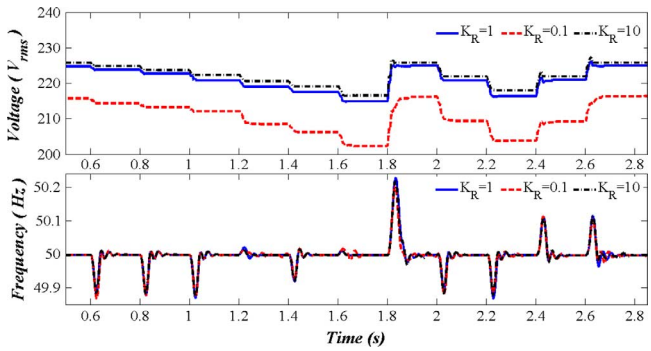

Fig. 5. System response for load disturbance with different values K_R (10: dotted, 0.1: dashed line, 1: solid).

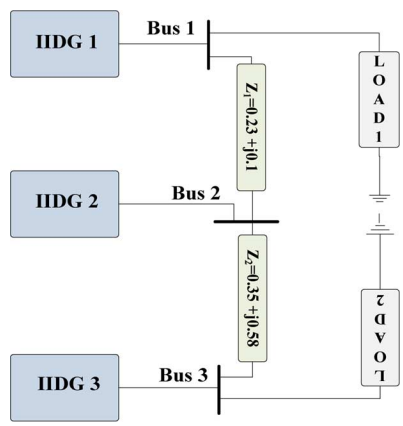

Fig. 6. MG with three DGs and two load banks.

is kept constant. Active and reactive loads are simultaneously decreased to primary values at 1.8 s.

Finally, for better recognizing of the GDC performance, in the final four steps, both active and reactive loads are changed together. The simulation results for different values of Z ($K_R = 0.1, K_R = 1$, and $K_R = 10$) are shown in Fig. 5. This figure shows that the proposed GDC method stabilizes the MG's frequency and voltage following the step load changes. It is also investigated that the developed control strategy is capable to maintain frequency and voltage stability even in more serious conditions.

IV. ANFIS-BASED GDC APPROACH

The main weak point of the proposed generalized droop control method in the previous section is in strong dependency of the approach to the line parameters (R and X). Consider a more complex MG which is shown in Fig. 6 [28]. The proposed technique is depending on the line parameters. The DGs (220 V, 50 Hz) are connected to two local load banks, at bus 1 and bus 3 [28]. System parameters are considered as given in Table I.

It is obvious that in this MG, unlike the simple MG (Fig. 3), relationship between generation and consumption is not accomplished only via one line. For example, DG source 2 shares its generation power between load 1 and load 2. Thus, between generation and consumption cannot be specified with a special resistance R and inductance X. In such cases, to achieve a desirable response, a virtual R and X should be considered in control structure of DG. According to the proposed control structure in the previous section, for a DG, a line should be existed between power source and load. Therefore, there are six line parameters

that must be determined ($[R_1X_1R_2X_2R_3X_3]$). Thus, in MGs with several DG units and loads, due to the existence of several lines in the system, the virtual line parameters should be used. But if the MG scales to be adequately large, the number of parameters, calculation time and also the possibility of stranding evolutionary algorithm in the local minimum will be considerable. Here, to solve this problem, an ANFIS unit is used instead of the GDC to meet same accuracy without any dependency to the MG structure.

A. ANFIS Controller Design

Adding the training ability of the ANN to the FL creates a new hybrid technique, known as ANFIS [29]. The ANFIS provides an adaptive modelling procedure to learn data set information. It creates an appropriate input/output (I/O) mapping with membership functions (MFs) based on fuzzy *If-Then* rules to generate the I/O pairs. The MFs parameters can be changed through the learning process.

Here, to determine the parameters, a hybrid learning algorithm is used. In this technique, the fuzzy rules updating is possible when the system is being trained, and by an appropriate ANN tuning, it does not require any previous knowledge about the MFs and rules. The MFs configuration depends on their parameters, and the ANFIS selects these parameters automatically. The fuzzy inference system (FIS) is built by using appropriate I/O data, which the parameters are set by means of the BP algorithm and the least square error (LSE) method.

In this study, the FIS has two inputs, active power (P) and reactive power (Q). The output is frequency (f) or voltage (V). If the rule base contains two fuzzy (if-then) rules of *Takagi-Sugeno*'s type, as follows:

1. If P is A_1 and Q is B_1, then $f_1 = p_1P + q_1Q + r_1$,
2. If P is A_2 and Q is B_2, then $f_2 = p_2P + q_2Q + r_2$.

Then, the corresponding equivalent ANFIS structure with five layers can be constructed as shown in Fig. 7. Following, the layers are explained in detail.

Layer 1: In the first layer, the input variables are applied to obtain the fuzzy sets proportional to the inputs variables. Every node i in this layer have a function that shows membership value of each input, so the node outputs can be described as

$$\begin{aligned} O_{1,i} &= \mu_{A_i}(P); \quad i = 1, 2 \\ O_{1,i} &= \mu_{B_{i-2}}(Q); \quad i = 3, 4 \end{aligned} \tag{18}$$

where, P or Q is the input to node i, A_i (or B_i) is a linguistic label (small, large, ...). In other words, $O_{1,i}$ is the MF of A_i. Usually μ_{A_i} is chosen in a bell-shaped form with maximum and minimum of 1 and 0, respectively. For example, here the $\mu_{A_i}(P)$ is chosen as follows

$$\mu_{A_i}(P) = \frac{1}{1 + \left(\frac{P - c_i}{\alpha_i}\right)^{2\beta}} \tag{19}$$

where, $\{\alpha_i, \beta_i, c_i\}$ is a parameter set known as premise parameters. Effect of changing these parameters on the MFs is shown in Fig. 8.

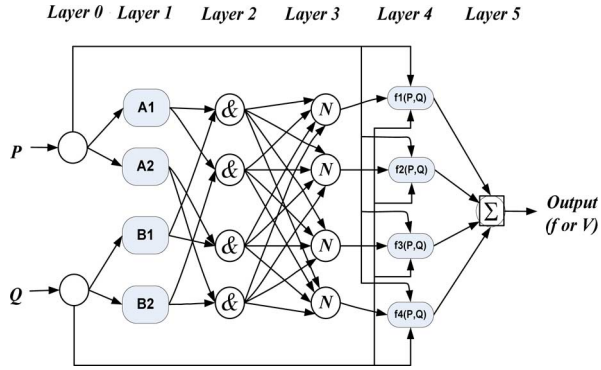

Fig. 7. Typical structure of an ANFIS.

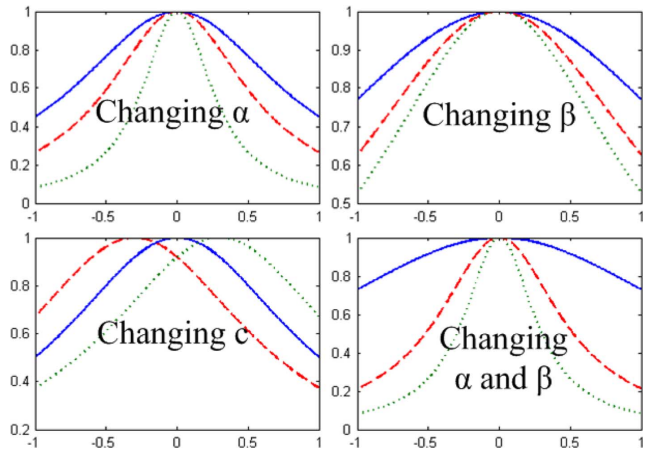

Fig. 8. Effect of changing parameters (α_i, β_i, c_i) on the MFs.

Layer 2: The second layer output is the multiplication of the incoming signals from layer 1. For example,

$$O_{2,i} = W_i = \mu_{A_i}(P) \times \mu_{B_i}(Q); \quad i = 1, 2 \tag{20}$$

where, W_i presents the firing strength of a rule. The incoming signals are equivalent to the antecedent (If) part of rules.

Layer 3: In this layer, the activity level of each rule is calculated. The number of layers is equal to the number of fuzzy rules. This layer output is a normalized form of the previous layer. The ith node calculates the ratio of ith rule's firing strength versus all rule's firing strengths, as described below.

$$O_{3,i} = \bar{w}_i = \frac{w_i}{\sum_j w_j} \tag{21}$$

Layer 4: The forth layer produces the partial output values. Output node i in this layer is *Takagi-Sugeno* type as follows

$$O_{4,i} = \bar{w}_i f_i = \bar{w}_i(p_i\mathrm{P} + q_iQ + r_i) \tag{22}$$

where, $\bar{w}_i$ is the output of *layer*. The $\{p_i, q_i, r_i\}$ is a parameters set, known as consequent parameters.

Layer 5: Finally, the ANFIS output is obtained from the fifth

layer. This single node computes the overall output as the summation of all incoming signals.

$$O_5 = \sum_i \bar{w}_i f_i \tag{23}$$

ANFIS uses two parameter sets: the premise parameters set $\{\alpha_i, \beta_i, c_i\}$, and the consequent parameters set $\{p_i, q_i, r_i\}$. The adjustment of these two parameter sets is a two-step process: *forward pass* and *backward pass*. First, in the *forward pass*, the premise parameters are fixed and the consequent parameters are computed using the LSE algorithm (off-line learning). Then, in the *backward pass*, the consequent parameters are fixed and the premise parameters are computed using the BP gradient decent algorithm.

To design the ANFIS-based controller, first the GDC structure, which is used in the simple MG (Fig. 3), might be modeled by the ANFIS. Then, after ensuring about the model validity, the proposed ANFIS-based controller could be used instead of the GDC block diagram (Fig. 2). Design steps can be summarized as follows:

i) By applying and testing the GDC on the system shown in Fig. 3, and then saving the controller inputs/outputs, the training data for the ANFIS controller synthesis are collected. To obtain an accurate model, the training data under violent changes of active and reactive loads are considered.

ii) After obtaining the training data set, the ANFIS structure to be completed. The MFs of input and output are considered in form of linear and Gaussian functions.

iii) Following creating the controller structure, using the optimal hybrid method (combination of the LSE and BP), the ANFIS is trained for 5 epochs (iterations) with a small error tolerance (i.e., 0.00001 ms).

B. Validity Evaluation

After designing the ANFIS-based GDC, the model validity should be investigated in view point of dynamic behavior similarity with the GDC unit. For this purpose, the I/O data set of $K_R = 1$ is used for training the ANFIS unit. As shown in Fig. 2, the GDC consists of two inputs and two outputs that are active/reactive power and frequency/voltage amplitude, respectively.

Since the ANFIS is a multi-input-single-output (MISO) system, two ANFIS structures should be separately used for frequency and voltage outputs. These controllers include two inputs and one output which. Since, it is expected that the ANFIS controllers must simulate the GDC behaviour as far as possible; the input data (active and reactive power) should cover a wide range of load changes. After generating the I/O data set, the ANFIS models are trained. Due to high switching frequency of the inverter (4000 Hz), the sampling time is considered as 100000 samples per second until the ANFIS-based controllers could be able to simulate the system behaviour, accurately.

To evaluate the ANFIS performance, both real and training data sets are considered as test data. The real and training data

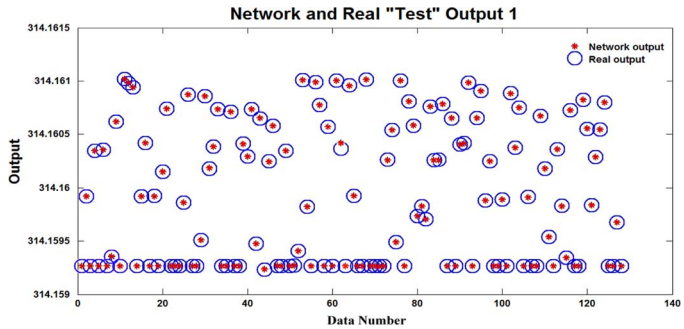

Fig. 9. Trained network output and real output.

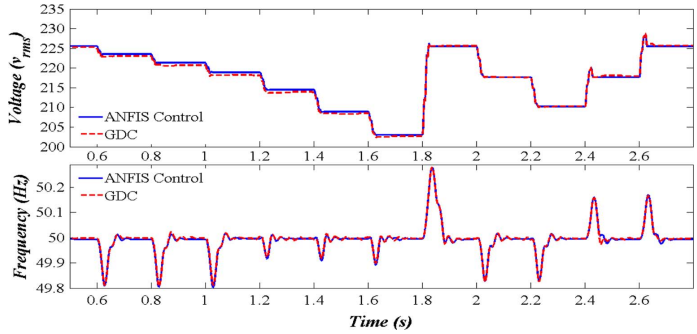

Fig. 10. Voltage and frequency under the violent changes of the load.

are compared together. Fig. 9 shows the ANFIS network outputs versus the real outputs. Comparison of real and network data shows that the training process is accurately done, and the ANFIS-based controllers have effectively simulated the GDC system behaviour. After replacing the GDC with the ANFIS trained controllers, under the violent changes of active and reactive loads, the system voltage and frequency are compared to the previous structure. The active and reactive power changes are considered same as shown in Fig. 4. Fig. 10 shows the validity of the ANFIS models.

V. Case Studies and Test Scenarios

A. 3-Bus Test MG

To test and verify the effectiveness of the proposed droop control method based on ANFIS controller; first the 3-bus MG shown in Fig. 6 with pure active loads are considered: 30 kW and 10 kW active loads at bus 1 and bus 3, respectively. Then, with occurring violent changes in both loads at different times, the impact of dynamic load changes with trained ANFIS controller on the MG performance is evaluated. The active and reactive load changes are shown in Table II. The system response including voltage and frequency profiles is shown in Fig. 11. This figure shows the capability of the proposed intelligent control for stabilizing the MG's voltage and frequency.

Now, consider the outage of a DG from the MG system, following an event. To see the voltage and frequency profiles after outage of a DG, and to check either the remained islanded MG is stable or not; DG1 is removed from the MG in time duration of 0.4 to 0.6 seconds. Simulation results for this scenario are shown in Figs. 12 and 13. After removing DG1 at t = 0.4 s,

TABLE II
LOAD CHANGE SCENARIO

Time duration [s]	Load 1 [kVA]	Load 2 [kVA]
0-0.3	30	10
0.3-0.5	30	j40
0.5-0.7	30 +j10	10
0.7-0.9	30	j10
0.9-1.1	0	10
1.1-1.3	30	10

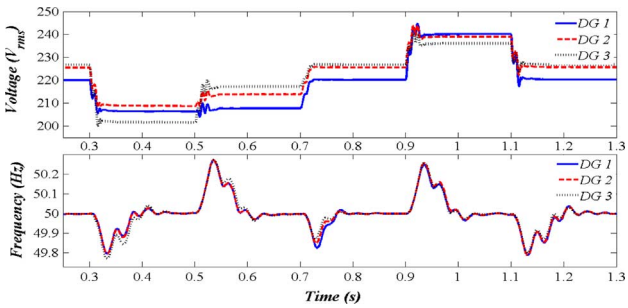

Fig. 11. Voltage and frequency profile under violent load changes.

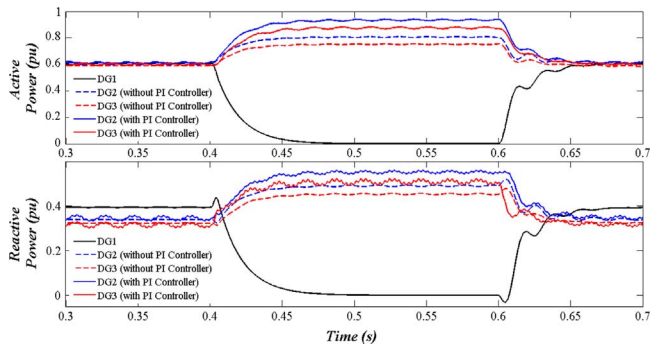

Fig. 12. Output active and reactive power affected by outage of DG 1.

other DGs are going to compensate the DG1 absence and stop the voltage/frequency deviation. When DG1 is removed, due to lack of secondary control loop, a steady droop is observed in the load voltage terminals. The steady voltage droop can be returned to the nominal operating value by adding a proportional-integral (PI) controller to the voltage control loop (see Figs. 12 and 13). This controller is not activated for the previous test scenario (Fig. 11).

B. 11-Bus Test MG

To prove the reliability of the closed-loop system with the designed ANFIS controller, it is also tested on an 11-bus test system, which is shown in Fig. 14 [30]. At times 0.3 s, 0.5 s and 0.7 s; a load change is occurred in buses 2, 5 and 8, respectively. The loads of the test system before 0.3 s are presented in Table III. This load change scenario is shown in Table IV. The voltage and frequency profile under this load change scenario are shown in Fig. 15.

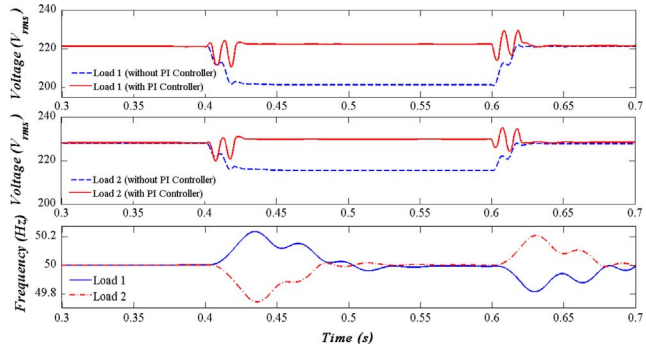

Fig. 13. Voltage/frequency profile of local loads following outage of DG 1.

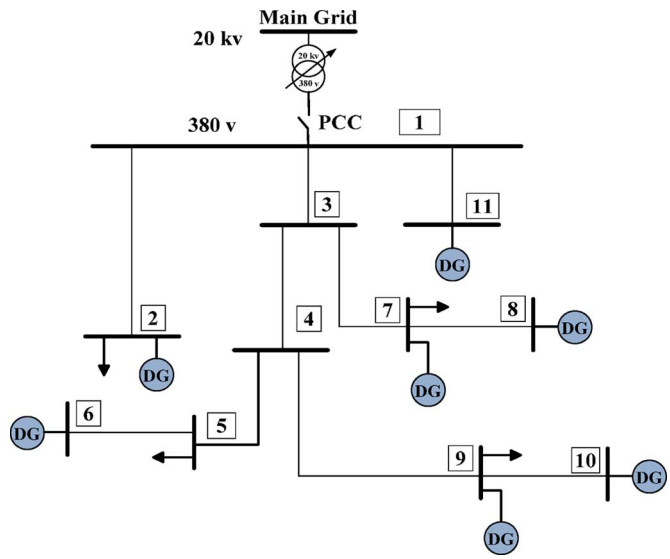

Fig. 14. 11-bus MG test system.

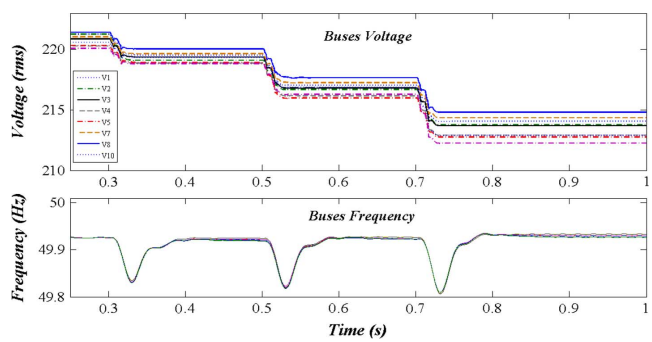

Fig. 15. Frequency and voltage response of 11 bus MG test system in the presense of load change scenario given in Table V.

TABLE III
LOADS IN 11-BUS MG TEST SYSTEM

Bus Number	Load (kVA)
2	20+j10
5	30
7	45
9	25+j10

TABLE IV
LOAD CHANGE SCENARIO FOR 11-BUS MG TEST SYSTEM

	Bus Number	Load Change (kVA)
at t=0.3s	2	10+j3
at t=0.5s	5	13+j5
at t=0.7s	9	16+j8

TABLE V
LOADS IN 14-BUS MG TEST SYSTEM

Bus Number	Load (kVA)
8	4.25+j2.63
9	15.58+j9.66
10	13.32+j8.25
12	20.45+j12.64
13	4.25+j2.63

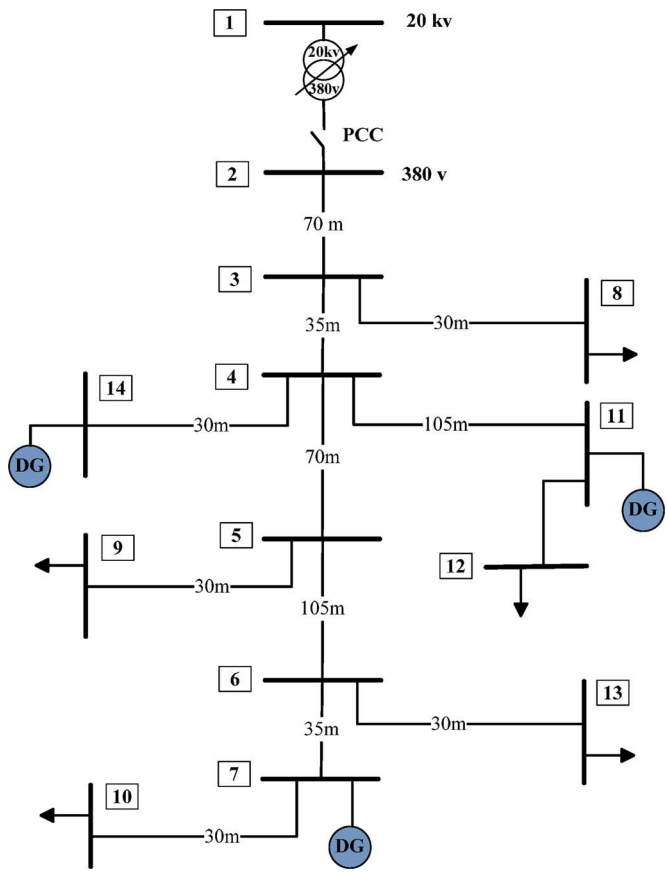

Fig. 16. 14-bus MG test system.

C. 14-Bus Test MG

To investigate the effectiveness of the proposed ANFIS droop controller; it is also examined on a 14-bus test system, which is shown in Fig. 16. This MG is a modified version of the given grid in [31]. At times 0.4 s, 0.6 s and 0.8 s; a load change is occurred in buses 8, 9, and 13, respectively. The loads of the test system before 0.4 s are presented in Table V. The load change scenario is shown in Table VI. The voltage and frequency profile under this load change scenario are shown in Fig. 17. The simulation results show that by the designed ANFIS-based GDC,

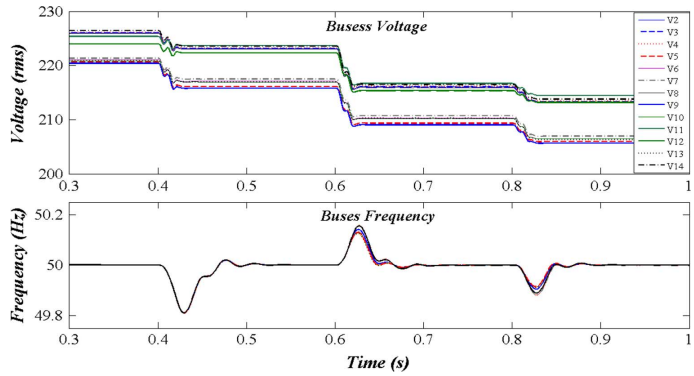

Fig. 17. Frequency and voltage response of 14-bus MG test system in the presense of load change scenario given in Table VII.

TABLE VI
LOAD CHANGE SCENARIO FOR 14-BUS MG TEST SYSTEM

	Bus Number	Load Change (kVA)
at t=0.4s	8	j7
at t=0.6s	9	7
at t=0.8s	13	3+j2

system stability with desirable performance is guaranteed under severe load changes.

VI. CONCLUSION

The present paper provides a solution for intelligent model-free based generalized droop control (GDC) synthesis for simultaneous voltage and frequency regulation in the islanded microgrids. A GDC is proposed based on the well-known conventional voltage/frequency droops. But the addressed GDC highly depends on the MG configuration and line parameters. To remove this dependency and propose a model-free based GDC, an adaptive neuro-fuzzy inference system (ANFIS) is developed. The ANFIS is responsible to simulate dynamic behavior of the GDC.

The proposed ANFIS is trained by a desired I/O data set of the GDC, and then it is applied to the inverter interfaced DG control structure. Using the developed intelligent GDC synthesis, one does not need more to know the MG structure and line parameters. Thus, this approach is applicable for a wide range of MGs. The effectiveness of the proposed method is examined on several test case systems.

REFERENCES

[1] R. Lasseter, A. Akhil, C. Marnay, J. Stephens, J. Dagle, R. Guttromson, A. Meliopoulous, R. Yinger, and J. Eto, "The CERTS microgrid concept," *White Paper for Transmission Reliability Program, Office of Power Technologies, US Department of Energy*, 2002.

[2] H. Bevrani, M. Watanabe, and Y. Mitani, "Microgrid controls," in *Standard Handbook for Electrical Engeneers*, H. W. Beaty, Ed., 16 ed. New York: McGraw Hill, 2012, Section 16.

[3] R. Lasseter, J. Eto, B. Schenkman, J. Stevens, H. Vollkommer, D. Klapp, E. Linton, H. Hurtado, and J. Roy, "CERTS microgrid laboratory test bed," *IEEE Transactions on Power Delivery*, vol. 26, pp. 325–332, 2011.

[4] C. Moreira and J. P. Lopes, "Microgrids dynamic security assessment," in *International Conference on Clean Electrical Power, 2007. ICCEP '07*, 2007, pp. 26–32.

[5] C. Schauder and H. Mehta, "Vector analysis and control of advanced static VAR compensators," in *Generation, Transmission and Distribution, IEE Proceedings C*, 1993, pp. 299–306.

[6] A. Yazdani and R. Iravani, "A unified dynamic model and control for the voltage-sourced converter under unbalanced grid conditions," *IEEE Transactions on Power Delivery*, vol. 21, pp. 1620–1629, 2006.

[7] P. Arboleya, D. Diaz, J. Guerrero, P. Garcia, F. Briz, C. Gonzalez-Moran, and J. G. Aleixandre, "An improved control scheme based in droop characteristic for microgrid converters," *Electric Power Systems Research*, vol. 80, pp. 1215–1221, 2010.

[8] K. Fujimoto, T. Ota, Y. Shimizu, T. Ichikawa, K. Yukita, Y. Goto, K. Ichiyanagi, T. Takeda, K. Hirose, and Y. Okui, "Load frequency control using storage system for a micro grid," in *Transmission & Distribution Conference & Exposition: Asia and Pacific, 2009*, 2009, pp. 1–4.

[9] T. Senjyu, E. Omine, M. Tokudome, Y. Yonaha, T. Goya, A. Yona, and T. Funabashi, "Frequency control strategy for parallel operated battery systems based on droop characteristics by applying H∞ control theory," in *Transmission & Distribution Conference & Exposition: Asia and Pacific, 2009*, 2009, pp. 1–4.

[10] S. K. Mishra, "Design-oriented analysis of modern active droop-controlled power supplies," *IEEE Transactions on Industrial Electronics*, vol. 56, pp. 3704–3708, 2009.

[11] J. M. Guerrero, L. G. de Vicuña, J. Matas, M. Castilla, and J. Miret, "A wireless controller to enhance dynamic performance of parallel inverters in distributed generation systems," *IEEE Transactions on Power Electronics*, vol. 19, pp. 1205–1213, 2004.

[12] T. Senjyu, Y. Miyazato, A. Yona, N. Urasaki, and T. Funabashi, "Optimal distribution voltage control and coordination with distributed generation," *IEEE Transactions on Power Delivery*, vol. 23, pp. 1236–1242, 2008.

[13] K. De Brabandere, B. Bolsens, J. Van den Keybus, A. Woyte, J. Driesen, and R. Belmans, "A voltage and frequency droop control method for parallel inverters," *IEEE Transactions on Power Electronics*, vol. 22, pp. 1107–1115, 2007.

[14] H. Bevrani and T. Hiyama, *Intelligent Automatic Generation Control*. : CRC PressI Llc, 2011.

[15] A. El-Keib and X. Ma, "Application of artificial neural networks in voltage stability assessment," *IEEE Transactions on Power Systems*, vol. 10, pp. 1890–1896, 1995.

[16] P. Subbaraj and K. Manickavasagam, "Generation control of interconnected power systems using computational intelligence techniques," *Generation, Transmission & Distribution, IET*, vol. 1, pp. 557–563, 2007.

[17] H. Bevrani, A. Ghosh, and G. Ledwich, "Renewable energy sources and frequency regulation: Survey and new perspectives," *Renewable Power Generation, IET*, vol. 4, pp. 438–457, 2010.

[18] P. Villenueve, "Concerns generated by islanding [electric power generation]," *Power and Energy Magazine, IEEE*, vol. 2, pp. 49–53, 2004.

[19] J. M. Guerrero, J. C. Vasquez, J. Matas, L. G. de Vicuña, and M. Castilla, "Hierarchical control of droop-controlled AC and DC microgrids—A general approach toward standardization," *IEEE Transactions on Industrial Electronics*, vol. 58, pp. 158–172, 2011.

[20] J. A. P. Lopes, C. Moreira, and A. Madureira, "Defining control strategies for microgrids islanded operation," *IEEE Transactions on Power Systems*, vol. 21, pp. 916–924, 2006.

[21] T. L. Vandoorn, B. Renders, L. Degroote, B. Meersman, and L. Vandevelde, "Active load control in islanded microgrids based on the grid voltage," *IEEE Transactions on Smart Grid*, vol. 2, pp. 139–151, 2011.

[22] E. Barklund, N. Pogaku, M. Prodanovic, C. Hernandez-Aramburo, and T. C. Green, "Energy management in autonomous microgrid using stability-constrained droop control of inverters," *IEEE Transactions on Power Electronics*, vol. 23, pp. 2346–2352, 2008.

[23] G. A. Diaz, C. Gonzalez-Moran, J. Gomez-Aleixandre, and A. Diez, "Scheduling of droop coefficients for frequency and voltage regulation in isolated microgrids," *IEEE Transactions on Power Systems*, vol. 25, pp. 489–496, 2010.

[24] M. B. Delghavi and A. Yazdani, "A unified control strategy for electronically interfaced distributed energy resources," *IEEE Transactions on Power Delivery*, vol. 27, pp. 803–812, 2012.

[25] M. B. Delghavi and A. Yazdani, "An adaptive feedforward compensation for stability enhancement in droop-controlled inverter-based microgrids," *IEEE Transactions on Power Delivery*, vol. 26, pp. 1764–1773, 2011.

[26] H. Bevrani, *Robust Power System Frequency Control*. : Springer, 2009.

[27] M. Liserre, R. Teodorescu, and F. Blaabjerg, "Stability of photovoltaic and wind turbine grid-connected inverters for a large set of grid impedance values," *IEEE Transactions on Power Electronics*, vol. 21, pp. 263–272, 2006.

[28] N. Pogaku, M. Prodanovic, and T. C. Green, "Modeling, analysis and testing of autonomous operation of an inverter-based microgrid," *IEEE Transactions on Power Electronics*, vol. 22, pp. 613–625, 2007.

[29] J. S. R. Jang, "ANFIS: Adaptive-network-based fuzzy inference system," *IEEE Transactions on Systems, Man and Cybernetics*, vol. 23, pp. 665–685, 1993.

[30] S. Papathanassiou, Study-Case LV Network [Online]. Available: http://microgrids.power.ece.ntua.gr/documents/Study-Case%20LV-Network.pdf [Online]. Available:

[31] S. Papathanassiou, N. Hatziargyriou, and K. Strunz, "A benchmark low voltage microgrid network," in *Proc. CIGRE Symp. "Power Systems With Dispersed Generation"*, Athens, Greece, Apr. 2005.

Hassan Bevrani (S'90-M'04-SM'08) received Ph.D. degree in electrical engineering from Osaka University, Osaka, Japan, in 2004. From 2004 to 2011, he has worked as a post-doctoral fellow, senior research fellow, visiting professor, and professor with Kumamoto University (Japan), Queensland University of Technology (Australia), Kyushu Institute of Technology (Japan) and Osaka University. Since 2000, he has been an Academic Member with the University of Kurdistan, Sanandaj, Iran. He is the author of 3 books, 10 book chapters, and about 150 journal/conference papers. His current research interests include smart grid operation and control, intelligent and robust control applications in power system and power electronic industry.

Shoresh Shokoohi (S'2011-M'2013) was born in Sanandaj, Kurdistan, Iran, on April, 1987. He received the B.Sc. (with honors) and the M.Sc. degrees in electrical engineering from the University of Kurdistan, in 2009 and 2012, respectively. In 2010, he was with the control laboratory of university of Kurdistan, as a lecturer. He then joined the Instrumentation and Control Unit (ICU) at the Iranian Oil Pipelines and Telecommunication Company (IOPTC). His current research interests are in areas of micro/smart Grids control and robust/intelligent control applications in power electronic industry.